Surface modification of upconverting nanoparticles by layer-by-layer assembled polyelectrolytes and metal ions

Emilia Palo*[,a,b,c], Mikko Salomäki[a,c], Mika Lastusaari[a,c]

[a] University of Turku, Department of Chemistry, FI-20014 Turku, Finland

[b] University of Turku Graduate School (UTUGS), Doctoral Programme in Physical and Chemical Sciences, Turku, Finland

[c] Turku University Centre for Materials and Surfaces (MatSurf), Turku, Finland

Corresponding author

*emilia.palo@utu.fi

KEYWORDS: layer-by-layer; nanoparticles; polyelectrolytes; lanthanides; $NaRF_4$; upconversion luminescence

ABSTRACT

Modificating and protecting the upconversion luminescence nanoparticles is important for their potential in various applications. In this work we demonstrate successful coating of the nanoparticles by a simple layer-by-layer method using negatively charged polyelectrolytes and neodymium ions. The layer fabrication conditions such as number of the bilayers, solution concentrations and selected polyelectrolytes were studied to find the most suitable conditions for the process. The bilayers were characterized and the presence of the desired components was studied and confirmed by various methods. In addition, the upconversion luminescence of the bilayered nanoparticles was studied to see the effect of the surface modification on the overall intensity. It was observed that with selected deposition concentrations the bilayer successfully shielded the particle resulting in stronger upconversion luminescence. The layer-by-layer method offers multiple possibilities to control the bilayer growth even further and thus gives promises that the use of upconverting nanoparticles in applications could become even easier with less modification steps in the future.

INTRODUCTION

In upconversion luminescence low energy radiation (usually near infra-red, NIR) is converted into higher energy radiation such as UV-vis range (300–700 nm)[1]. This can be obtained using combinations of lanthanide ions such as Yb^{3+}-Er^{3+} or Yb^{3+}-Tm^{3+}. It has several potential applications ranging from medical imaging [2] and biomedical assays [3] into wavelength conversion in solar cells [4] and enhancement of photosynthesis [5]. Especially the biomedical applications benefit from the low autofluorescence of upconversion materials and the possibility to use challenging matrices such as whole blood which limits the use of conventional UV excited labels because of its strong absorption below 600 nm [3]. Using

$NaYF_4$ as a host material is common because of its hexagonal structure (β-NaRF4; $P6_3/m$ (#176), Z: 1.5 [6, 7]) that has superior upconversion luminescence compared to that of the cubic structure (α-$NaRF_4$; $Fm\bar{3}m$ (#225), Z: 2 [7]) [6, 8]. Although, the hexagonal structure has the strongest upconversion luminescence it still has some major drawbacks such as low quantum yield and considerable quenching of upconversion luminescence when in direct contact with water [9, 10].

Recently, the research on these materials has focused on shielding the upconversion luminescence of the materials by creating core-shell structures to prevent quenching by surface defects and water or cross-relaxation processes between used lanthanide ions [11, 12]. Shielding the upconversion materials, especially those used in biomedical applications, is vital because their tendency to disintegrate in solutions and thus quenching the luminescence [13, 14]. In addition, neodymium has been studied as an absorber instead of ytterbium because of the advantages it has in biomedical use. These advantages involve shifting the excitation wavelength from 980 to 808 nm resulting deeper penetration range in the tissue and less overheating due to laser absorbance [15–17]. Neodymium is then transferring the absorbed excitation energy through the lattice via Yb^{3+} ions that are more efficient in feeding the emitting ions (*e.g.* Er^{3+} or Ho^{3+}). This can be done with using core-shell structure having absorbing and emitting ions at the close range [18] or introducing an inert energy migration layer between the layers where the absorbing Nd^{3+} and emitting ion are located [19]. Using neodymium as an absorber alongside with ytterbium could also benefit having more absorption lines to gather energy more efficiently for the upconversion.

One option to coat wide range of different materials is to prepare oppositely charged layers with layer-by-layer method [20–22]. This method has been used for coating solid surfaces and creating thin bilayer films of polymers but it is also possible to use it for coating nanoparticles [23–25]. The bilayers are usually made with oppositely charged

polyelectrolytes but it is also possible to build them with negatively charged polyelectrolyte and positive metal ions as a cationic component [26, 27].

Different polymers and surfactants have been studied with upconversion nanoparticles partly because of their effect on nanoparticles colloidal stability, but also because they help the further use in biomedical field by adding more contacting sites to attach linking components. One of the remaining problems is that the intensity of upconversion luminescence quenches significantly when surfactants are used and the particles are introduced into aqueous solvents [28]. Recently, it was demonstrated that coating $NaYF_4:Yb^{3+},Tm^{3+}$ nanoparticles by poly(acrylic acid) enabled attachment of Cu^{2+} onto the particle surface which subsequently was able to coordinate into molecules [29]. To the authors' knowledge no investigations has been made to see how the layer-by-layer formation on to the nanoparticle surface using metal cations (in our case lanthanide ions) and polyelectrolytes is obtained. Also it was in our interest to observe if the upconversion luminescence can be maintained or even enhanced by using the lanthanide ions as sensitizers in bilayer assemblies on the material surface, thus mimicking the core-shell structure.

In this work, the upconverting β-$NaYF_4:Yb^{3+},Er^{3+}$ nanoparticles synthesized with a modified [30] high-temperature co-precipitation synthesis [31] were coated with either polyphosphate (PP) or poly(acrylic acid) (PAA) and Nd^{3+} ions to form bilayers. Both of the polyelectrolytes were primarily chosen because of their probability to adhere on neodymium ions, but also because of polyphosphates possibility to enhance the luminescence properties [32] and the use of poly(acrylic acid) in further modifying the particles for applications [33]. The number of bilayers and the (ionic) concentrations of used solutions were studied to see how they affect the formation of bilayers.

EXPERIMENTAL SECTION

Reagents. Potassium polyphosphate (PP, potassium metaphosphate $(KO_3P)_n$, ABCR), Poly(acrylic acid) ($M_w \approx 100{,}000$, PAA, $(C_3H_4O_2)_n$, 35 wt-% in H_2O, Aldrich), sodium chloride (NaCl 99.5 %, J.T. Baker), rare earth(III) chloride hexahydrate ($RCl_3 \cdot 6H_2O$ R: Y, Yb, Er 99.99% and Nd 99.9 % purity with respect to other rare earths, Sigma-Aldrich) and hydrochloric acid (HCl 37 % puriss p.a., Sigma-Aldrich). Absolute ethanol was used as received.

Materials preparation. The β-$NaYF_4$:Yb^{3+},Er^{3+} nanomaterials were prepared with the synthesis procedure reported previously [30] using dopant concentrations of x_{Yb}: 0.17 and x_{Er}: 0.03. Coating solutions were prepared with 5/10/20 mM (monomer concentration of polyelectrolytes) of polyelectrolyte (polyphosphate or poly(acrylic acid)) solubilized in aqueous solution of 0.05, 0.1 or 0.2 M NaCl. Similarly, an aqueous solutions of 5/10/20 mM $NdCl_3 \cdot 6H_2O$ were prepared in quartz distilled H_2O. pH of the solutions was unadjusted and *ca*. 5.

Removal of the oleic acid surface. The oleic acid was removed from the nanoparticle surface with a modified procedure [29, 34] where nanoparticles were suspended in 1 ml of absolute ethanol and the pH was adjusted with concentrated HCl (pH < 2). Suspension was ultrasonicated for 60 minutes and after that centrifuged (50 000*g*, 10 min). The procedure was repeated twice. Oleate free nanoparticles were then dried in a desiccator for further characterization.

Layer-by-layer coating of the nanoparticles. The coating cycle of the core particles involved the particles (dry powder, *ca*. 50 mg) to be dispersed in the desired coating solution (usually 10 mM of polyelectrolyte, referring to monomer concentrations (PAA, PP) or $NdCl_3$,

total volume 1 ml), ultrasonicated for two minutes and then collected via centrifuging (50 000*g*, 10 min). After removing the coating solution the particles were washed two times to remove unattached material using quartz distilled H_2O and collected via centrifuging. The charged layers were deposited in similar manner until desired amount of bilayers was achieved. After the final layer the nanoparticles were dried in a desiccator and characterized.

Characterization The core particle structure was determined at room temperature with the X-ray powder diffraction (XRD) using a Huber G670 image plate Guinier camera (Cu $K_{\alpha 1}$ radiation, 1.5406 Å) with a 2θ range of 4-100° (step 0.005°). Data collection time was 30 min and 10 data reading scans of the image plate. From this data the crystallite size of the core material was calculated with the Scherrer formula [35] using reflections (002) and (200) for the thickness and width of the hexagonal faces, respectively. The particle morphologies were determined with a JEM-1400 Plus transmission electron microscope (TEM) equipped with OSIS Quemesa 11Mpix bottom mounted digital camera. The used acceleration voltage was 120 kV or 40 kV depending on the grid used. Before the measurements the samples were prepared dispersing the nanomaterials into ethanol and then drying a drop on the surface of a copper grid (120 kV) or graphene oxide coated copper grid (40 kV).

The presence of the polyelectrolytes was studied with Fourier transformed infrared spectra (FT-IR) using Bruker Vertex 70 using MVP Star Diamond setup using 32 scans between 450 and 4500 cm^{-1}. The resolution was 4 cm^{-1}. The surface ions were probed with reflection spectra measured using Avantes Avaspec-2048×14 fiber spectrometer between 350 and 1000 nm. As a light source a 60 W incandescent light bulb was used and the measurements were done with integration time of 400 ms and 30 scans. The elemental composition of the products was studied with X-ray fluorescence spectroscopy (XRF) using PANanalytical Epsilon 1 apparatus using its internal Omnian calibration with an average of four scans. The

qualitative thermal behavior of the layered materials was studied with one measurement per sample using a TA Instruments SDT Q600 TGA-DSC apparatus. The measurements were made between 35 and 600 °C with heating rate of 10 °C/min using flowing air sphere (100 ml/min). The error for weight in this setup is *ca*. 1 %. Zeta potential for studying the layer formation was measured using Malvern Zetasizer Nano-ZS equipment with three parallel measurements. The concentration of aqueous solutions was 100 μg/ml with pH of *ca*.6.

The upconversion luminescence spectra with 973 nm excitation were measured at room temperature with an Avantes Avaspec HS-TEC spectrometer using the average of 20 scans. A fiber-coupled continuous NIR laser diode IFC-975-008-F (Optical Fiber Systems) with 973 nm (10 270 cm^{-1}) was used as an excitation source with current power of 5000 mA. Dry nanomaterials were held inside a rotating capillary tube. After the sample a short-pass filter with a cutoff of 750 nm (Newport) was used to exclude excitation radiation. The emission was collected at a 90° angle to the excitation and directed to the spectrometer with an optical fiber. For the 808 nm excited upconversion luminescence a continuous NIR fiber laser WSLX-808-004-H (Wave spectrum) at 808 nm (12 380 cm^{-1}) was used as an excitation source with current power of 4500 mA. The measurement system and conformation were the same as with the measurements done with 973 nm excitation with an exception that after the sample a 700 nm filter (Newport) was used.

RESULTS AND DISCUSSION

Defining the core particles

The core nanoparticles were successfully prepared with previously reported synthesis method using 1-octadecene and oleic acid [30] and were of pure hexagonal form (Figure 1). The average crystallite size of the used β-$NaYF_4$:Yb^{3+},Er^{3+} core material was 22±1 nm for the h00 and 29±2 nm for the 00l planes (Table S1). TEM images of the core nanoparticles revealed

that they are evenly sized and nearly spherical which makes them good candidates for the layering process as the surface is equal for possible attaching sites. The removal of the oleic acid on the as-prepared particle surface before the layer-by-layer treatments was confirmed by FT-IR measurements (Figure S1). The distinguishable vibrations of oleic acid between 1400-1500 cm^{-1} [34] have disappeared from the washed materials suggesting successful removal of the oleic acid surfactant. It is possible that some un-capped oleic acid is still present in the dried material as small amounts of C-H vibrations are visible near 2900 cm^{-1}.

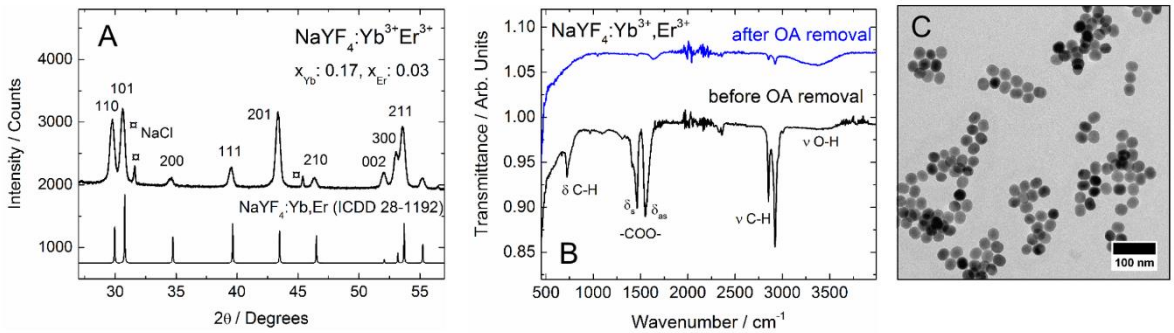

Figure 1. The X-ray diffraction pattern with a hexagonal reference [7] (A), FT-IR spectra before and after the oleic acid (OA) removal (B) and a TEM image (C) of the nanoparticles used as a core material. The scale bar represents 100 nm.

Investigating the layer-by-layer formation

The formation of the polyelectrolyte-neodymium bilayers was studied by various methods as in most cases only either part of the studied bilayer was visible.

From the FT-IR spectra of the materials coated with poly(acrylic acid), the fingerlike vibrations of PAA ranging from 1000 to 1750 cm^{-1} could be observed with all of the materials that should contain the polyelectrolyte (Figure 2, S2) [36]. These vibrations were also distinguishable from those of oleic acid when the unwashed oleic acid capped material is compared to the layered materials. The C-H vibrations at 2900 cm^{-1} were observed with all materials, but they are also present in the spectra of the core material indicating that even

195 though the characteristic oleic acid vibrations are nearly invisible there might be traces of it
196 left. When the core materials were layered by polyphosphate (PP), vibrations from the
197 polyelectrolytes shifted to lower wavenumbers being at 900-1400 cm^{-1}. These vibrations were
198 present in all of the materials that should contain polyphosphate. With increasing amount of
199 bilayers it seemed that the vibrations for polyelectrolytes grew stronger which could indicate
200 that there is increasing amount of polyelectrolytes on the surface.

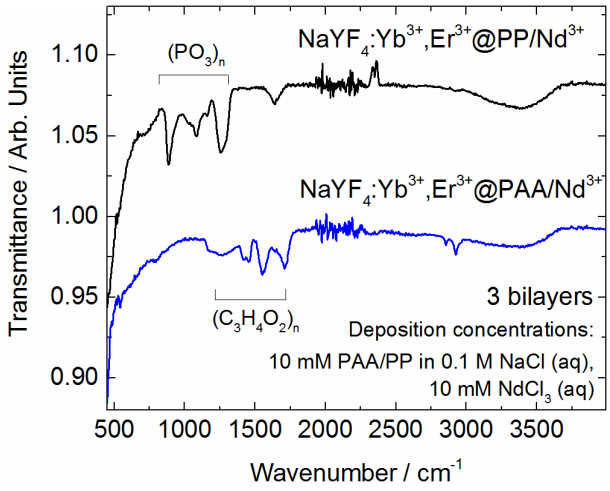

201

202 **Figure 2.** FT-IR spectra of the $NaYF_4:Yb^{3+},Er^{3+}$ with three bilayers of PP/Nd^{3+} or PAA/Nd^{3+}
203 prepared with deposition concentrations of 10 mM PAA/PP in 0.1 M NaCl (aq) and 10 mM
204 $NdCl_3$ (aq).
205
206 The lanthanides have distinguishable absorption bands from each other. This makes it
207 possible to probe the lanthanides present in the material surface using reflectance
208 spectroscopy. The core materials have absorption bands that can be pointed directly either to
209 Er^{3+} (490, 520, 540 650 and 800 nm) and Yb^{3+} (975 nm) ions. After the layer-by-layer
210 process absorptions that can be assigned for Nd^{3+} ions (575, 740, 795 and 870 nm) arise.
211 When the reflection spectra was normalized to Yb^{3+} absorption it was observed that the
212 absorption lines specific to neodymium increased with increasing amount of bilayers while
213 the absorptions that can be pointed to Er^{3+} remained the same or weakened (Figure 3, S3).

This suggests that there is increasing amount of neodymium present on the surface when the amount of bilayers is increasing.

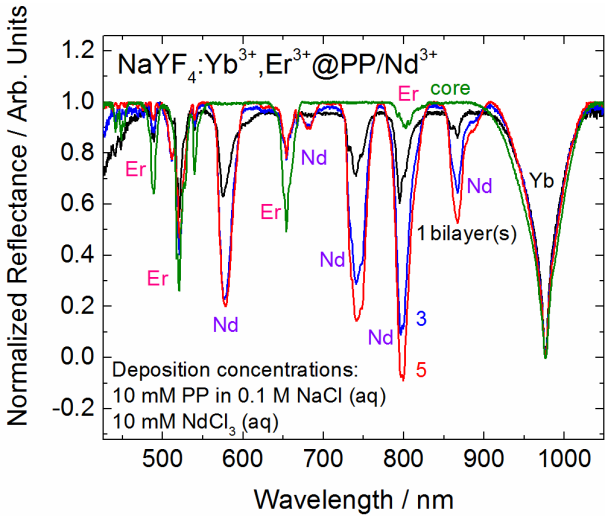

Figure 3. Reflectance spectra of the $NaYF_4$:Yb^{3+},Er^{3+} core and 1, 3 and 5 bilayers of PP/Nd^{3+} prepared with deposition concentrations of 10 mM PP in 0.1 M NaCl (aq) and 10 mM $NdCl_3$ (aq).

From the X-ray fluorescence spectroscopy it was possible to confirm the presence of the neodymium in the materials. Using different ionic strengths of NaCl for polyelectrolyte solutions in the layering process the difference in the amount of attached neodymium could be observed when compared to yttrium amount. It seemed that using 0.1 M ionic concentration of NaCl would be optimal for getting the maximum amount of Nd^{3+} ions on to the surface (Figure 4A, Table S2-S3). The pH of the polyelectrolyte solutions is expected to play more important role in the loading of Nd^{3+} ions than the ionic concentration because the latter only affects the packing of the polyelectrolyte chain [37] whereas the pH affects to the ionization of the polyelectrolyte chain. However, as the polyelectrolyte chain opens it could offer more attaching sites for Nd^{3+} ions compared to more compact chain which might result this increase. When the nanoparticles were coated by polyphosphate the amount of phosphor on the surface could also be seen increasing with increasing amount of bilayers from the XRF

but the results are not as reliable as for the lanthanides since the phosphor is either out of the detection range of the equipment or the amount of phosphor is too low for efficient detection during the first bilayers. This could be observed from the materials that had polyphosphate related vibrations in the IR spectra but no phosphor observed in the XRF. However, it seemed that also for the layering of the polyphosphate the 0.1 M NaCl is optimal ionic concentration.

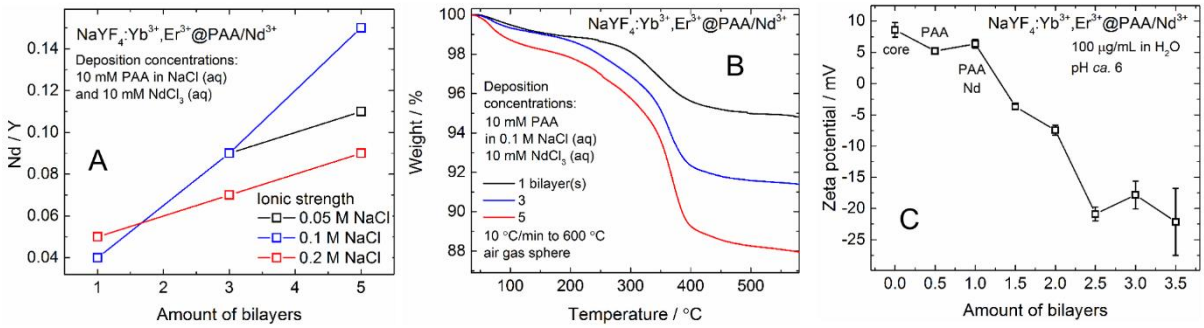

Figure 4. XRF analysis (A), thermal analysis (B) and zeta potential (C) of the $NaYF_4:Yb^{3+},Er^{3+}$@PAA/Nd^{3+} with different amount of bilayers.

Thermal analysis was used to observe the poly(acrylic acid) on the nanoparticle surface as it can be burned off using an artificial air sphere while the particle itself still remains intact at 500 °C. With increasing amount of PAA the weight loss was larger suggesting successful layering of the nanoparticles (Figure 4B, S4). If the weight loss was plotted against the layering cycles it could be seen that as with the other methods, ionic concentration of 0.1 M NaCl is the most effective in forming bilayers. Thermal analysis was also made from the materials where the layering was studied within half bilayers (Figure S5). From those curves it could be observed that when the polyelectrolyte layer is introduced the weight loss increases. When the complementary positively charged ion layer is added the weight loss decreases suggesting that the Nd^{3+} ions are now present in the bilayer and remain in the sample pan as the polyelectrolyte is burned off. If the materials were layered with PP there were no significant changes in the mass curve of the nanoparticles as it remained unchanged

during the heating. However, it was observable that there were still some organic residues especially in the first bilayers of the materials, as well as different amounts of interlocked water residue due to the layering cycles.

The zeta potential measurements were made to probe the success of the layering cycles as both anionic and cationic components should be visible during the measurement. In comparison to the core nanoparticle zeta potential there was a decrease in zeta potential already within the first negative polyelectrolyte layer as well as the expected rise for the complementary positive neodymium layer (Figure 4C). The drop after each added polyelectrolyte layer was larger than the subsequent rise, suggesting that even though the positive ions are added on to the surface there is not enough of them to overpower the overall larger negative charge coming from the polyelectrolyte. Having the zeta potential varying only little during the first two bilayers also indicates that the polyelectrolyte layers might not cover the particle fully until the third polyelectrolyte layer is introduced at 2.5 bilayers.

Finally, the possible aggregation of the nanoparticles during the layering cycles was studied with TEM imaging with the materials layered with PAA and neodymium. The increasing amount of bilayers or the modification of the ionic concentration of the polyelectrolyte solutions did not seem to have a great effect in the nanoparticle aggregation and they seem to be mostly independent (Figure 5). However, the possible layers of PAA are not clearly distinguishable from the images even though the nanoparticle surface seems to get blurry and could indicate that there are some changes. To get further look on the PAA layers an additional imaging was made with lower voltage (40 kV) using graphene oxide copper grids. From this image the PAA layer can be seen more clearly (Figure 5, S6) being *ca*. 2 nm with the material having three bilayers. It also shows that even though the nanoparticles do not

look aggregated in the TEM images with higher voltage, there is probably also some interlocked particles obtained after the layering. Also the graphene oxide grid can have an effect in aggregating or piling the particles together that is not seen in the other images.

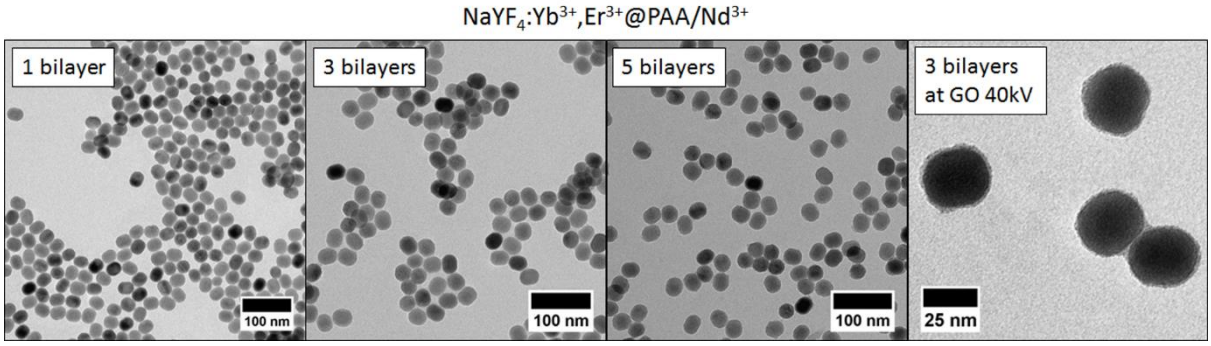

Figure 5. TEM images of the $NaYF_4:Yb^{3+},Er^{3+}$@PAA/Nd^{3+} with 1, 3 and 5 bilayers prepared with deposition concentrations of 10 mM PAA in 0.1 M NaCl (aq) and 10 mM $NdCl_3$ (aq). The scale bar represents 100 (1, 3 and 5 bilayers with 120 kV) and 25 nm (3 bilayers with 40 kV).

Effect of the deposition concentrations

The differences in the bilayer formation with modified polyelectrolyte and neodymium concentrations was studied by preparing only one bilayer on top of the nanoparticles. Both of the used component concentrations were varied between 5, 10 and 20 mM while keeping the other unmodified at 10 mM. The ionic concentration of polyelectrolyte solutions was kept at 0.1 M with NaCl.

The FT-IR spectra showed no significant change in any of the vibrations of the materials made with modified concentrations, only the specific vibrations of PAA and PP were present as they are with the materials having more bilayers (Figure S3). However, with the reflection spectra there was more variation in the neodymium absorption within the materials (Figure

6). With both polyelectrolytes it seemed that lowering the neodymium concentration to 5 mM weakened the absorption indicating that there were less neodymium present on the surface.

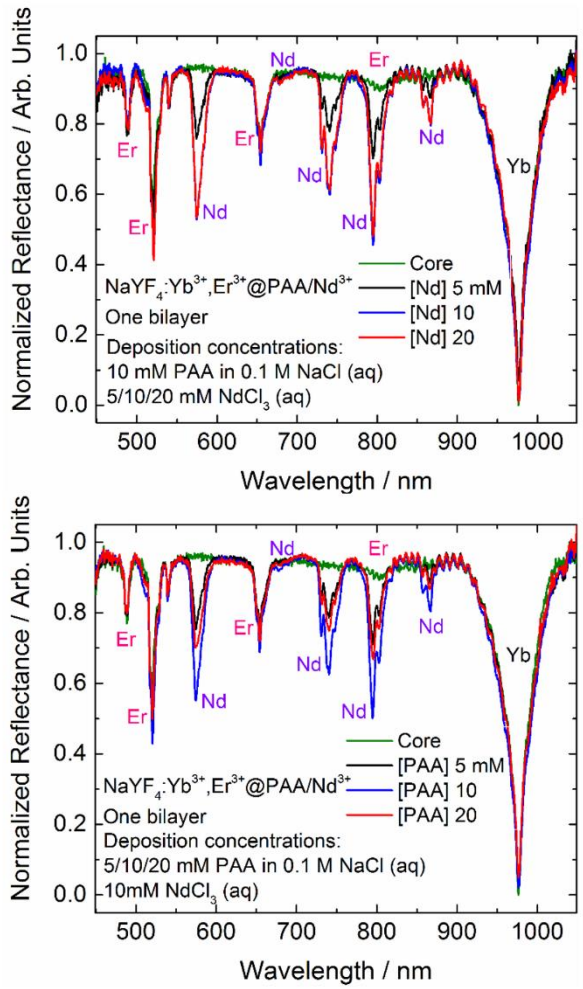

Figure 6. Reflectance spectra of the $NaYF_4$:Yb^{3+},Er^{3+} core and one bilayer of PAA/Nd^{3+} prepared with deposition concentrations of 5, 10 and 20 mM while keeping the other fixed at 10 mM.

However, with increasing the concentration to 20 mM there is no more increase. This could mean that there is no more available binding sites left for the neodymium ions in the polyelectrolyte matrix even though there are more ions present in the solution. Using PAA as a polyelectrolyte it seemed that having 10 mM concentration was the most efficient in attaching neodymium ions. With the 5 and 20 mM PAA concentration the absorption lines of

Nd^{3+} were much weaker. With PP there was a slight increase in neodymium absorption throughout the increase in the polyelectrolyte concentration.

The XRF analysis of the materials prepared with modified concentrations confirm the same observations as with the reflectance spectra. Thermal analysis of the materials using PAA with modified neodymium concentrations showed that there was a slight decrease in the weight loss suggesting the increasing amount of neodymium present. Also when the PAA concentration was modified there was an increase in the weight loss indicating the increasing amount of polyelectrolyte in the materials. With materials layered using PP there were no self-evident trends that could indicate anything on the properties of the layers.

Investigating the luminescence properties

As the core nanoparticles have upconversion luminescence properties the effect of the layering to its emission intensity was studied by both 973 and 808 nm excitation. When the upconversion was excited through the Yb^{3+} ions with the 973 nm (10 280 cm^{-1}) excitation the ionic strength of the used polyelectrolyte played a crucial role. Using PAA with 0.05 M NaCl the luminescence intensity weakens with increasing amount of bilayers. However, with higher ionic strength the luminescence obtained from the all bilayers is stronger than from the core materials suggesting that the layering protects the core particle sufficiently to hinder the energy loss from the surface (Figure 7, S7). This protection is probably due to the more dense packed polyelectrolytes as a result of the increasing ionic strength and their ability to cover the surface more efficiently thus removing possible H_2O and COO^- groups resulting in enhanced luminescence. Neodymium ions do not have energy levels corresponding with the 973 nm excitation so they are unlikely to absorb the excitation energy before it gets to the core. However, they have strong probability to absorb the emission obtained from erbium and

offer non radiative routes resulting in loss of upconversion luminescence when the amount of bilayers is increased.

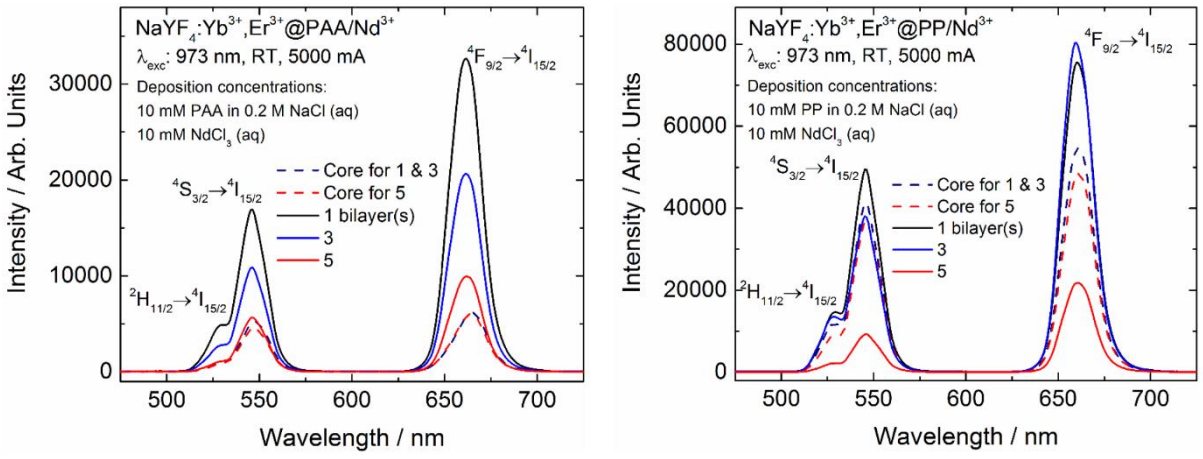

Figure 7. Upconversion luminescence spectra excited with 973 nm of the $NaYF_4:Yb^{3+},Er^{3+}$ nanoparticles with bilayers of PAA/Nd^{3+} (left) and PP/Nd^{3+} (right) prepared with deposition concentrations of 10 mM PAA/PP in 0.2 M NaCl (aq) and 10 mM $NdCl_3$ (aq).

With the PP bilayers it seemed that with all ionic strengths used the upconversion luminescence is increased after the first bilayer but increasing the bilayer amount results in weakening luminescence (Figure 7). This enhancement has been observed also in other luminescent particles such as $ZnS:Mn^{2+}$ and is due to surface passivation of the nanoparticles [32]. It seems that the protection of the polyelectrolyte layer is competing with the energy transfers, and thus energy loss, made possible by Nd^{3+} ions in the surface [38]. This is due to obtaining upconversion luminescence within the core materials Yb^{3+}-Er^{3+} energy transfer. The competition to gain the visible upconversion luminescence arises from the large surface-to-volume ratio of the nanoparticles along with the probability of the Yb-Yb energy migration within the nanoparticles to the surface [10]. This energy migration could result in losing the upconversion luminescence to any impurities present at the nanoparticle surface instead of visible luminescence from Er^{3+}. So the neodymium ions might have an double role,

either act as an absorber of the obtained emission or preventing the possibility for the migrating energy to find the emitting ion altogether.

The deposition concentrations had an impact on the obtained upconversion luminescence intensity and the 10 mM concentration yielded the strongest emission in all cases. However, when one bilayer was prepared by the ions used in the core lattice a straightforward trend was observed with both polyelectrolytes used. With inert yttrium the upconversion luminescence is strongest suggesting good shielding of the upconversion luminescence energy transfer processes (Figure 8). This is in good agreement with the core-shell material studies where the shell is manufactured from the same fluoride material as the core [16, 39]. Also when the active ions, ytterbium and erbium, were added to the bilayer a similar enhancement in upconversion luminescence was observed. With yttrium the enhancement was strongest and with ytterbium weakest. This could be expected due to the facts that the ytterbium is in charge of the energy transfer processes in upconversion luminescence and it can absorb the excitation energy before it gets to the upconverting core. The same applies for erbium even though it seems that its probability to absorb the excitation is weaker or that some of the absorbed energy is again converted to emission. However, yttrium does not have energy levels interacting with excitation nor emission pathways making the luminescence more efficient.

This emphasizes the suggestion that the quenching with increasing bilayers could be a result from the increasing amount of neodymium ions absorbing either the upconversion luminescence obtained from erbium or via non-radiative routes before finding the emitting erbium ions. However, the interplay between the shielding properties of polyelectrolyte layers and the quenching properties of neodymium ions is still unclear and needs further investigations in the future.

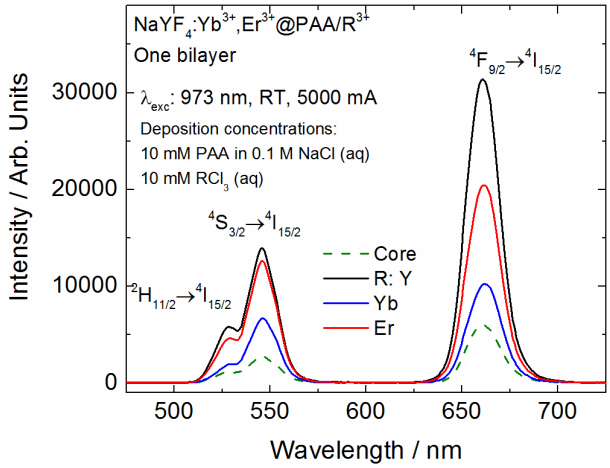

Figure 8. Upconversion luminescence spectra excited with 973 nm of the $NaYF_4:Yb^{3+},Er^{3+}$ nanoparticles with bilayers of PAA/R^{3+} (R: Y, Yb, Er) prepared with deposition concentrations of 10 mM PAA in 0.1 M NaCl (aq) and 10 mM RCl_3 (aq).

The upconversion luminescence excited by 808 nm (12 380 cm^{-1}) was studied to see if the addition of neodymium could provide an alternative route to excite the upconversion materials. With varying ionic strength the upconversion luminescence obtained from the layered materials is weaker than by the core materials itself. The upconversion luminescence can also be seen to weaken with increasing amount of bilayers (Figure S8). This suggests that the increasing amount of Nd^{3+} ions on the surface structure is absorbing the excitation and losing it through non-radiative relaxation pathways. The decrease is not as intense with materials layered by PAA than those with PP on the surface.

With the varying concentrations of deposition solutions no trends were observed with the 808 nm excited upconversion luminescence and the overall luminescence obtained was weak. When the core ions were layered with the polyelectrolytes it could be observed that there is an increase in the upconversion luminescence obtained from the materials. The enhancement was similar with both polyelectrolytes and with all ions used suggesting that the enhancement probably arises only from the surface protection of the materials because of the used ions only erbium has energy levels to match the excitation energy.

The data obtained does not give possibility to confirm mechanism of the observed quenching. However, as the neodymium itself has wide range of energy levels it is possible that parts of excited energy is lost through non radiative pathways. In the future more investigations to determine the reason for the energy loss is needed.

CONCLUSIONS

A successful new surface modification of the upconverting nanoparticles was possible using the simple layer-by-layer method using negatively charged polyelectrolytes and positively charged neodymium ions. In addition, the upconversion luminescence intensity of the core particles was increased with selected layering parameters. These surface modifications of the nanoparticles give new insight not just for the future of luminescent particle design but also adds a new chapter to layer-by-layer designs. Using the layer-by-layer method brings multiple possibilities to vary layering further by either changing the conditions of the polyelectrolytes or varying the positively charged component and offers the possibility to eliminate steps needed for bioconjugation in biomedical use [3].

Taking the studied conditions into consideration, the ionic strength of 0.1 M was the most efficient in producing the bilayers with both polyelectrolytes and neodymium as they can be seen increasing in the materials after increasing bilayers. Modifying the solution concentration did not have any significant effect on the formed bilayers. However, it seems that with PAA as the polyelectrolyte the concentration of 10 mM is the optimum if one considers the amount of the attached neodymium on the surface.

Using PAA as the polyelectrolyte it was possible to enhance the upconversion luminescence excited with 973 nm with selected layering parameters. This is due to shielding of the surface and thus preventing the energy losses from the surface impurities. Similar enhancement was observed with small number of bilayers of PP. However, the PP itself does not give further

attaching sites to conjugate the particles for applications. For this reason using PAA on the surface would be more suitable for further applications [33]. Using neodymium in the bilayers did not give the desired energy transfer with the 808 nm excitation even though upconversion luminescence could be observed from the materials.

In the future, the knowledge gained from this research will be used to optimize the layering process further and the mechanisms behind the upconversion processes in these systems will be investigated in detail. Also to benefit from the surface modifications in the biomedical use, thorough investigations to ensure the stability of the bilayer modifications will be carried out.

SUPPLEMENTARY INFORMATION

Supplementary information including additional characterization data for the materials such as FT-IR spectra, reflection spectra, XRF results, thermal analysis, TEM images and upconversion luminescence spectra can be found in the online version.

ACKNOWLEDGEMENT

Financial support from the Academy of Finland project “NOMSEC” and the Vilho, Yrjö and Kalle Foundation is gratefully acknowledged. Eerik Salonen is thanked for the preliminary studies of polyelectrolyte and rare earth ion interactions. The preceding work of Iko Hyppänen with the upconversion measurement equipment is gratefully acknowledged. Ermei Mäkelä is thanked for the help during the zeta potential measurements and Markus Peurla for the TEM images. This work made use of the Laboratory of Electron Microscopy premises at University of Turku.

REFERENCES

[1] F. Auzel, Upconversion and Anti-Stokes Processes with f and d Ions in Solids, Chem. Rev. 104 (2004) 139–173.

[2] M. Ylihärsilä, E. Harju, R. Arppe, L. Hattara, J. Hölsä, P. Saviranta, et al., Genotyping of clinically relevant human adenoviruses by array-in-well hybridization assay, Clin. Microbiol. Infect. 19 (2013) 551–557.

[3] R. Arppe, L. Mattsson, K. Korpi, S. Blom, Q. Wang, T. Riuttamäki, et al., Homogeneous Assay for Whole Blood Folate Using Photon Upconversion, Anal. Chem. 87 (2015) 1782–1788.

[4] G. Bin Shan, H. Assaaoudi, G.P. Demopoulos, Enhanced performance of dye-sensitized solar cells by utilization of an external, bifunctional layer consisting of uniform β-$NaYF_4:Er^{3+}Yb^{3+}$ nanoplatelets, ACS Appl. Mater. Interfaces. 3 (2011) 3239–3243.

[5] T. Antal, E. Harju, L. Pihlgren, M. Lastusaari, T. Tyystjärvi, J. Hölsä, et al., Use of near-infrared radiation for oxygenic photosynthesis via photon up-conversion, Int. J. Hydrogen Energy. 37 (2012) 8859–8863.

[6] K.W. Krämer, D. Biner, G. Frei, H.U. Güdel, M.P. Hehlen, S.R. Lüthi, et al., Hexagonal Sodium Yttrium Fluoride Based Green and Blue Emitting Upconversion Phosphors, Chem. Mater. 16 (2004) 1244–1251.

[7] PCPDFWIN v 1.30, Powder Diffraction File, 1997, International Centre for Diffraction Data, entries 06-0342 (cubic $NaYF_4$) and 28-1192 (hexagonal $Na(Y_{0,57}Yb_{0,39}Er_{0,04})F_4$).

[8] I. Hyppänen, J. Hölsä, J. Kankare, M. Lastusaari, L. Pihlgren, T. Soukka, Preparation and Up-Conversion Luminescence Properties of $NaYF_4:Yb^{3+},Er^{3+}$ Nanomaterials, Terrae Rarae. 16 (2009) 1–6.

[9] J.C. Boyer, F.C. van Veggel, Absolute quantum yield measurements of colloidal $NaYF_4:Er^{3+},Yb^{3+}$ upconverting nanoparticles, Nanoscale. 2 (2010) 1417–1419.

[10] R. Arppe, I. Hyppanen, N. Perälä, R. Peltomaa, M. Kaiser, C. Würth, et al., Quenching of the upconversion luminescence of $NaYF_4:Yb^{3+},Er^{3+}$ and $NaYF_4:Yb^{3+},Tm^{3+}$ nanophosphors by water: the role of the sensitizer Yb^{3+} in non-radiative relaxation., Nanoscale. 7 (2015) 11746–11757.

[11] Y. Wang, L. Tu, J. Zhao, Y. Sun, X. Kong, H. Zhang, Upconversion Luminescence of β-$NaYF_4:Yb^{3+},Er^{3+}$@β-$NaYF_4$ Core/Shell Nanoparticles: Excitation Power Density and Surface Dependence, J. Phys. Chem. C. 113 (2009) 7164–7169.

[12] N.J.J. Johnson, A. Korinek, C. Dong, F.C.J.M. Van Veggel, Self-focusing by Ostwald Ripening : A Strategy for Layer-by- Layer Epitaxial Growth on Upconverting Nanocrystals, J. Am. Chem. Soc. 134 (2012) 11068–11071.

[13] S. Lahtinen, A. Lyytikäinen, H. Päkkilä, E. Hömppi, N. Perälä, M. Lastusaari, et al., Disintegration of Hexagonal $NaYF_4:Yb^{3+},Er^{3+}$ Upconverting Nanoparticles in Aqueous Media: The Role of Fluoride in Solubility Equilibrium, J. Phys. Chem. C. 121 (2017) 656–665.

[14] O. Plohl, M. Kraft, J. Kovac, B. Belec, M. Ponikvar-Svet, C. Würth, et al., Optically Detected Degradation of $NaYF_4$:Yb,Tm-Based Upconversion Nanoparticles in Phosphate Buffered Saline Solution, Langmuir. 33 (2017) 553–560.

[15] R. Weissleder, A clearer vision for in vivo imaging, Nat. Biotechnol. 19 (2001) 316–317.

[16] X. Xie, N. Gao, R. Deng, Q. Sun, Q. Xu, X. Liu, Mechanistic investigation of photon upconversion in Nd^{3+}-sensitized core-shell nanoparticles., J. Am. Chem. Soc. 135 (2013) 12608–11.

[17] Y. Wang, G. Liu, L. Sun, J. Xiao, J. Zhou, C. Yan, Nd3+-Sensitized Upconversion Nanophosphors : Efficient In Vivo Bioimaging Probes with Minimized Heating Effect, ACS Nano (2013) 7200–7206.

[18] D. Chen, L. Liu, P. Huang, M. Ding, J. Zhong, Z. Ji, Nd^{3+}-Sensitized Ho^{3+} Single-Band Red Upconversion Luminescence in Core−Shell Nanoarchitecture, J. Phys. Chem. Lett. 6 (2015) 2833–2840.

[19] K. Prorok, A. Bednarkiewicz, Energy Migration Up-conversion of Tb^{3+} in Yb^{3+} and Nd^{3+} Codoped Active-Core/Active-Shell Colloidal Nanoparticles, Chem. Mater. 28 (2016) 2295–2300.

[20] G. Decher, Fuzzy Nanoassemblies: Toward Layered Polymeric Multicomposites, Science 277 (1997) 1232–1237.

[21] M.M. De Villiers, D.P. Otto, S.J. Strydom, Y.M. Lvov, Introduction to nanocoatings produced by layer-by-layer (LbL) self-assembly, Adv. Drug Deliv. Rev. 63 (2011) 701–715.

[22] J. Borges, J.F. Mano, Molecular Interactions Driving the Layer-by-Layer Assembly of Multilayers, Chem. Rev. 114 (2014) 8883–8942.

[23] G. Schneider, G. Decher, Functional core/shell nanoparticles via layer-by-layer assembly. Investigation of the experimental parameters for controlling particle aggregation and for enhancing dispersion stability, Langmuir. 24 (2008) 1778–1789.

514 [24] X. Hong, J. Li, M. Wang, J. Xu, W. Guo, J. Li, et al., Fabrication of magnetic
515 luminescent nanocomposites by a layer-by-layer self-assembly approach, Chem. Mater.
516 16 (2004) 4022–4027.

517 [25] K.S. Mayya, B. Schoeler, F. Caruso, Preparation and organization of nanoscale
518 polyelectrolyte- coated gold nanoparticles, Adv. Funct. Mater. 13 (2003) 183–188.

519 [26] M. Salomäki, M. Räsänen, J. Leiro, T. Huti, M. Tenho, J. Lukkari, et al., Oxidative
520 inorganic multilayers for polypyrrole film generation, Adv. Funct. Mater. 20 (2010)
521 2140–2147.

522 [27] M. Salomäki, O. Myllymäki, M. Hätönen, J. Savolainen, J. Lukkari, Layer-by-layer
523 assembled oxidative films as general platform for electrodeless formation of conducting
524 polymers, ACS Appl. Mater. Interfaces. 6 (2014) 2325–2334.

525 [28] S. Wilhelm, M. Kaiser, C. Würth, J. Heiland, C. Carrillo-Carrion, V. Muhr, et al.,
526 Water dispersible upconverting nanoparticles: effects of surface modification on their
527 luminescence and colloidal stability., Nanoscale. 7 (2015) 1403–1410.

528 [29] Q. Mei, H. Jing, Y. Li, W. Yisibashaer, J. Chen, B. Nan, Biosensors and Bioelectronics
529 Smartphone based visual and quantitative assays on upconversional paper sensor,
530 Biosens. Bioelectron. 75 (2016) 427–432.

531 [30] E. Palo, M. Tuomisto, I. Hyppänen, H.C. Swart, J. Hölsä, T. Soukka, et al., Highly
532 Uniform Up-Converting Nanoparticles: Why You Should Control Your Synthesis Even
533 More, J. Lumin. 185 (2017) 125–131.

534 [31] F. Wang, Y. Han, C.S. Lim, Y. Lu, J. Wang, J. Xu, et al., Simultaneous phase and size
535 control of upconversion nanocrystals through lanthanide doping, Nature. 463 (2010)
536 1061–1065.

[32] A.A. Bol, A. Meijerink, Luminescence Quantum Efficiency of Nanocrystalline ZnS:Mn^{2+}. 1. Surface Passivation and Mn2+ Concentration, J. Phys. Chem. B. 105 (2001) 10197–10202.

[33] B. Liu, Y. Chen, C. Li, F. He, Z. Hou, S. Huang, et al., Poly(Acrylic Acid) Modification of Nd^{3+} -Sensitized Upconversion Nanophosphors for Highly Efficient UCL Imaging and pH-Responsive Drug Delivery, Adv. Funct. Mater. 25 (2015) 4717–4729.

[34] N. Bogdan, F. Vetrone, G.A. Ozin, J.A. Capobianco, Synthesis of ligand-free colloidally stable water dispersible brightly luminescent lanthanide-doped upconverting nanoparticles, Nano Lett. 11 (2011) 835–840.

[35] H.P. Klug, L.E. Alexander, X-ray Powder Diffraction Procedures, Wiley, New York, 1959.

[36] J. Workman, Jerry, The Handbook of Organic Compounds: NIR, IR, Raman and UV-VIS Spectra Featuring Polymers and Surfactants, Academic Press, 2001.

[37] P. Chodanowski, S. Stoll, Polyelectrolyte Adsorption on Charged Particles in the Debye-Hueckel Approximation. A Monte Carlo Approach, Macromolecules. 34 (2001) 2320–2328.

[38] N.J.J. Johnson, S. He, S. Diao, E.M. Chan, H. Dai, A. Almutairi, Direct Evidence for Coupled Surface and Concentration Quenching Dynamics in Lanthanide-doped Nanocrystals, J. Am. Chem. Soc. 139 (2017) 3275–3282.

[39] G. Yi, G. Chow, Water-Soluble $NaYF_4$Yb,Er(Tm)/$NaYF_4$/Polymer Core Shell/Shell Nanoparticles with Significant Enhancement of Upconversion Fluorescence, Chem. Mater. 19 (2007) 341–343.

560 **GRAPHICAL ABSTRACT**

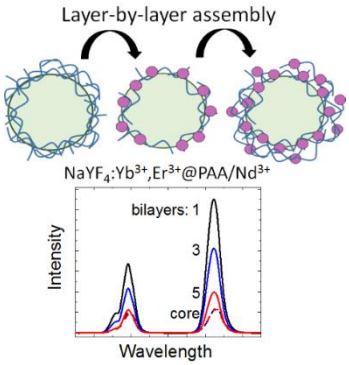

561